Available online on 15.06.2019 at http://jddtonline.info

Journal of Drug Delivery and Therapeutics

Open Access to Pharmaceutical and Medical Research

Open Access Research Article

Emerging Novel Drug Delivery System for Control Release of Curcumin through Sodium Alginate/Poly(ethylene glycol) Semi IPN Microbeads-Intercalated with Kaolin Nanoclay

O. Sreekanth Reddy[1]*, M.C.S Subha[1], T. Jithendra[1], C. Madhavi[2], K. Chowdoji Rao[2]

[1] Department of Chemistry, Sri Krishnadevaraya University, Ananthapuramu-515003, India
[2] Department of Polymer Science and Technology, Sri Krishnadevaraya University, Ananthapuramu-515003, India

ABSTRACT

The aim of the present work is fabrication of Curcumin encapsulated microbeads from Sodium Alginate/Polyethylene Glycol/Kaolin using glutaraldehyde as crosslinker by simple ionotropic gelation technique. The developed microbeads were characterized by Fourier transform infrared spectroscopy to confirm the formation of microbeads. Differential scanning calorimetry and X-ray diffraction studies have confirmed uniform molecular dispersion of CUR in the microbeads. Encapsulation efficiency of CUR in microbeads was ranged from 40 to 49%. Dynamic swelling studies and *in vitro* release kinetics were performed in simulated intestinal fluid (pH 7.4) and simulated gastric fluid (pH 1.2) at 37 °C. The results suggest that both swelling studies and cumulative release studies were depend on pH of the test medium, which might be suitable for intestinal drug delivery. The *in vitro* release data were analysed by using Korsmeyer peppas equation to compute the diffusion exponent (n); the results suggest that it followed non-Fickian diffusion.

Keywords: Sodium Alginate, Polyethylene Glycol, Kaolin, Microbeads, Drug delivery

Article Info: Received 28 April 2019; Review Completed 29 May 2019; Accepted 01 June 2019; Available online 15 June 2019

Cite this article as:

Sreekanth Reddy O, Subha MCS, Jithendra T, Madhavi C, Chowdoji Rao K, Emerging Novel Drug Delivery System for Control Release of Curcumin through Sodium Alginate/Poly(ethylene glycol) Semi IPN Microbeads-Intercalated with Kaolin Nanoclay, Journal of Drug Delivery and Therapeutics. 2019; 9(3-s):324-333
http://dx.doi.org/10.22270/jddt.v9i3-s.2847

***Address for Correspondence:**

O. Sreekanth Reddy, Research Scholar, Department of Chemistry, Sri Krishnadevaraya University, Ananthapuramu-515003, India

1. INTRODUCTION

During the last few years, a wide range of clay minerals have been used in pharmaceutical and biomedical fields exclusively for controlled drug delivery systems. Clay minerals are the oldest earth material composed of hydrous aluminium phyllosilicates which are usually formed as a product of chemical weathering of other silicate minerals at the surface of the earth[1]. Clay minerals are widely employed in the pharmaceutical industry as a lubricant, flavour correctors, desiccants, disintegrants, diluents, binders, pigments and opacifiers[2,3]. Clay minerals used as oral treatment of diarrhea and also for topical dermatological applications[4,5]. Clay minerals act as an active ingredient in pharmaceutical formulations because it can control the efficiency and consistency in dosage formulations and also improve the bioavailability because of their larger specific surface area and considerable ion-exchange capacity which attribute to their ability to control the efficiency of bio active molecules. Kaolin is a hydrated a two-dimensional (2D) aluminosilicate mineral[6,7]. It has been extensively used in biomedical related applications such as an activating agent for blood clotting[8], as an ingredient for operation haemostasis[9] and also used in drug delivery systems for prolonged release, especially of basic drugs because it can acts as active excipient in pharmaceutical dosage forms to increase the efficiency and bioavailability of drug molecules[10].

Sodium alginate (SA) is a natural polysaccharide comprising of β-D-mannuronic acid (M) and α-L-guluronic acid (G) repeating units linked by 1→4 linkage and displayed in the form of homo-polymeric (MMMM or GGGG blocks) and hetero-polymeric sequences (MGMGMG or GMGMGM blocks)[11]. Alginates have been used in pharmaceutical applications as a binder, viscosity modifying agent, stabilizer, tablet disintegrant and thickening agent. Alginates possess mucoadhesive biomaterial which could show a potential advantage in mucosal drug delivery due to its cytocompatibility, biocompatibility and biodegradation[12,13]. Advantage of alginates is used as a matrix for the fabrication of controlled and sustained release formulations because it is degraded and absorbed by the body during and after release of drug molecules without any toxic effects[14]. Therefore

alginate is a suitable matrix for sustained release of various drug molecules.

Poly Ethylene Glycol (PEG) is one of the most used polymer in emerging field of polymer based drug delivery. PEG is a widely used biomaterial due to its hydrophilicity, biocompatibility, and elimination via both renal and hepatic pathways[15]. PEG used as an inactive ingredient in the pharmaceutical industry as lubricants for medical devices, plasticizer, and as vehicles in dermatological applications suppositories, ointment and tablets[16,17]. Bendels et al. has reported that PEG showed elevated permeability in weak acids and neutral compounds but lowered permeability in weak bases[18]. Therefore, PEG has great profound influences on the intestinal absorption and systemic exposure of oral drugs. Hence PEG has been used in various applications such as drug delivery[19], tissue engineering[20] and in regenerative medicine[21].

Curcumin is a yellow bioactive compound extracted from the rhizome of turmeric (Curcuma longa)[22], possesses a wide range of pharmacological exploits including anti-inflammatory[23], anti-oxidant[24], antimicrobial[25], antirheumatic[26], thrombosis suppressing[27] and also it enhance anti-tumour activity against different types of cancer cells, including cancers of the colon, prostate, and breast[28,29]. Its biomedical applications are limited due to its poor solubility and rapid metabolism, which results in poor bioavailability. So, the main aim of the present study is to increase the bioavailability and encapsulation efficiency of curcumin, for this we have fabricated Kaolin intercalated Sodium Alginate/Polyethylene Glycol blend microbeads (Scheme 1). The developed microbeads were analysed by different techniques such as FTIR, XRD, DSC, TGA and SEM. Dynamic swelling studies and drug release kinetics were investigated in both simulated intestinal fluid (pH 7.4) and simulated gastric fluid (pH 1.2) at 37 °C and the results has been addressed.

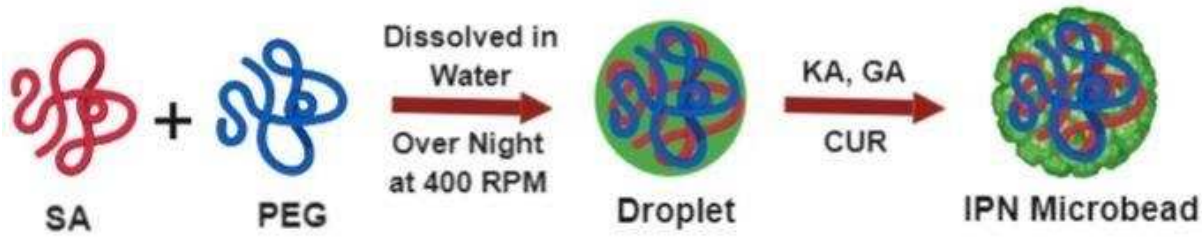

Scheme 1. Schematic representation of SA/PEG/KA blend IPN microbeads

EXPERIMENTAL

2.1. Materials

Kaolin was purchased from Sigma–Aldrich (USA). Sodium alginate, Polyethylene Glycol, Glutaraldehyde and Calcium Chloride, were purchased from Sd.Fine Chemicals, Mumbai, India. Curcumin was purchased from Loba Chemicals, Mumbai, India. Water used was of high purity grade after double distillation.

2.2. Preparation of Sodium Alginate/Mmt Microbeads:

Varying amounts of SA and PEG (as per given in Table 1) were weighed and dissolved in water under constant stirring overnight. To this solution, required amounts of Kaolin and Glutaraldehyde (as per given in Table 1) were added and stirred well. A required amount of Curcumin was added and stirred to obtain a homogeneous solution. Afterwards the suspension was placed 5mins for sonication to get homogenous suspension. There after the resulting suspension was slowly dropped into $CaCl_2$ solution, where the spherical beads formed instantly were kept for 40 min. The obtained wet beads were collected by decantation, washed three times with double distilled water to remove the drug attached on the bead surface, and finally were dried in air overnight at room temperature.

Table 1. Formulation and composition of all samples

Formulation code	SA (mg)	PEG (mg)	Distilled Water (mL)	Drug (mg)	GA (mL)	Kaolin (mg)
SP1	400	00	20	100	1	000
SP2	320	80	20	100	1	000
SP3	280	120	20	100	1	000
SP4	320	80	20	100	1	200
SP5	320	80	20	100	1	400
SP6	320	80	20	100	1	600
SP7	320	80	20	00	1	000

2.3. Characterizations Methods

2.3.1 Intercalation kinetics

To find out the maximum time required of CUR for intercalation with KA, intercalation kinetics experiment was performed. Weighed accurately 50 mg of CUR and 100 mg of KA, were dissolved in 20 mL of double distilled water with continuous stirring at 37 °C. At predetermined time intervals i.e., 0.25, 0.5, 1, 2, 4, 6, 8, 10, 14 hr, the drug solution was filtered and concentration of CUR was assayed by using UV spectrophotometer at fixed λ-max value of 470.00 nm.

2.3.2. Fourier Transform Infrared (FTIR) Spectral Analysis

Fourier-Transmission IR (FT-IR) spectra of PEG, SA, CUR, KA, Placebo microbeads, drug loaded SA/PEG microbeads and drug loaded SA/PEG/KA microbeads were measured as pellets in KBr with a FT-IR spectrophotometer (model Bomem MB-3000, with Horizon MB™ FTIR software) in the wavelength range of 400–4000 cm^{-1} to find out the possible chemical interactions between polymers and drug.

2.3.3. Differential Scanning Calorimetry (DSC)

DSC curves of CUR, Placebo microbeads, and drug loaded SA/PEG microbeads were recorded using Thermogravimetry analyzer Rheometric Scientific, Model DSC-SP, UK. The analysis was performed by heating the sample from 40 to 600 °C at the heating rate of 10°C/min under nitrogen atmosphere.

2.3.4. Thermogravimetric Analysis (TGA)

Thermogravimetric analysis of CUR, KA, Placebo microbeads, drug loaded SA/PEG microbeads and drug loaded SA/PEG/KA microbeads were carried out using Thermogravimetry analyzer Rheometric Scientific, Model DSC-SP, UK. About 12-14 mg of sample was placed into alumina crucible and the thermo grams were recorded between 40°C to 600°C at a heating rate of 10°C/min under nitrogen atmosphere.

2.3.5. X-Ray Diffraction (XRD) Analysis

The X-ray diffraction of pristine CUR, placebo microbeads, and drug loaded SA/PEG microbeads were performed by a wide angle X-ray scattering diffractometer (Panalytical X-ray Diffractometer, model-X'pert Pro) with CuKα radiation (λ= 1.54060) at a scanning rate of 10°/min to determine the crystallinity.

2.3.6. Scanning Electron Microscopy (SEM) Analysis

The topographical structure of microbeads was observed by using SEM (JOEL MODEL JSM 840A) with an accelerated voltage of 20 kV equipped with an EDAX detector.

2.3.7. Swelling behaviour

The swelling behaviour of different formulations was determined gravimetrically in simulated intestinal fluid (pH 7.4) and simulated gastric fluid (pH 1.2) at 37 °C. For this, 40mg of dry beads were suspended in 30ml of the buffer solutions at 37°C and their weight change was examined at different time intervals. This process is continued until the weight of swollen beads reached constant value. The % swelling degree was calculated by the following equation:

$$\% \text{ swelling degree} = \frac{\text{Weight of wet beads} - \text{Weight of dry beads}}{\text{Weight of dry beads}} \times 100$$

2.4. Encapsulation Efficiency

To investigate the encapsulation efficiency of CUR, a known mass of drug loaded microbeads (50mg) were immersed into 100mL of phosphate buffer solution (pH 7.4 containing 5% absolute ethyl alcohol) for 24 hr and then crushed the beads to ensure the complete extraction of CUR from the microbeads and filtered through filter paper. The filtered drug solution was assayed by ultraviolet spectrophotometer at the λ-max of 470.00 nm with placebo microbeads were used as a blank correction. Concentration of drug was determined by using calibration curve constructed by series of CUR standard solutions. Percentage of encapsulation efficiency was determined by the following formula.

$$\%EE = \frac{\text{CUR total used (mg)} - \text{CUR in the bath (mg)}}{\text{CUR total used (mg)}} \times 100$$

2.5. In Vitro Drug Release Studies

In vitro drug release studies were carried out by using a dissolution tester apparatus (Lab India, Mumbai, India) equipped with eight baskets at 37°C. Weighed 100 mg of the CUR loaded microbeads were taken in a dialysis bags for the drug release studies. The % release of CUR from microbeads was carried out in 900 mL of phosphate buffer solution pH7.4 and pH 1.2 at a rotation speed of 50 rpm to replicate intestinal and gastric fluid atmosphere respectively. At regular intervals of time, 5 mL aliquot samples were withdrawn, and analyzed using UV spectrophotometer at fixed λ-max value of 470.00 nm. After sample withdrawn, the same amount of fresh buffer at the same temperature was added to the release medium to maintain the sink condition. The released drug amount was obtained by using concentration versus absorbance calibration curve.

3.0. RESULTS AND DISCUSSIONS

3.1. Intercalation kinetics

Fig. 1 shows the intercalation kinetics of CUR with KA. From the results of intercalation kinetics, it was concluded that 16.93% of CUR was intercalated with KA through electrostatically within 2 hr and remains constant up to 14 hr. Therefore we should keep 2 hr time for intercalation of CUR with KA to avoid partial interaction.

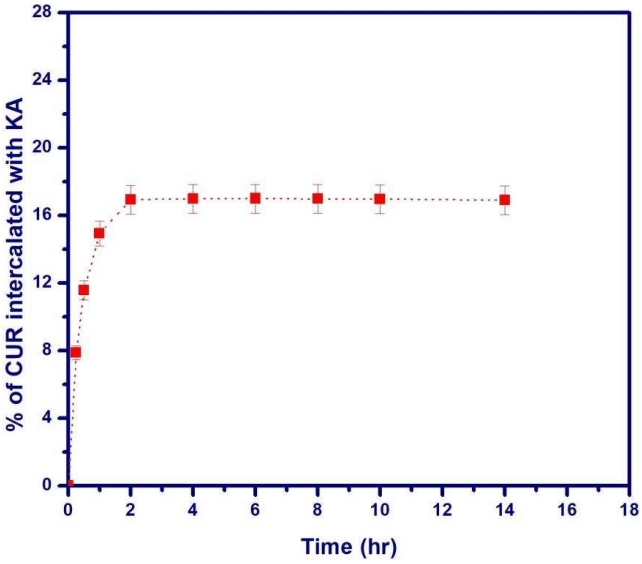

Fig. 1. Effect of time for Intercalation of CUR with KA

3.2. FTIR Spectral Analysis

The formation of microbeads was confirmed by FTIR spectroscopy. FTIR spectra of pure KA (a), SA (b), PEG (c), CUR (d), placebo micro beads (e), drug loaded SA/PEG micro beads (f) and drug loaded SA/PEG/KA micro beads (g) were represented in Fig. 2. The FTIR spectra of KA (Fig. 2a) shows a characteristic peaks at 3688 and 3625 cm^{-1} corresponds to O – H stretching frequency of Si – OH and Al – OH respectively, a peak at 3456 cm^{-1} assigned to H – O – H stretching frequency of interlayer water, peak at 2360 cm^{-1} was attributed to C – H stretching frequency, peak at 1596 cm^{-1} corresponds to O – H adsorbed water, the absorption bands at 1126 and 902 cm^{-1} corresponds to Si – O – Si stretching band [30]. The prominent peaks for SA (Fig. 2b) were 3416 cm^{-1} for O-H stretching frequency, 1388 cm^{-1} and 1612 cm^{-1} for the asymmetric and symmetric stretching frequency of carboxylate group C – O respectively. The FTIR

spectra of PEG (Fig. 2c) shows a characteristic absorption bands at 3464, 2877, 1469, 1350 and 1108 cm^{-1} corresponds to O – H stretching frequency, C – H stretching frequency, C – H bending, O – H bending and C – C, C – O stretching frequency respectively[31]. The FTIR spectra of CUR (Fig. 2d) shows a characteristic broad peak at 3496 cm^{-1} assigned to phenolic O–H stretching vibrations, a band at 2923 cm^{-1} corresponds to aromatic C–H stretching vibrations, a band at 1594 cm^{-1} for stretching vibration of benzene ring skeleton, a band at 1511 cm^{-1} corresponds to mixed (C=O) and (C=C) vibration, a band at 1272 cm^{-1} assigned to Ar-O stretching vibrations[32].

The FTIR spectra of placebo microbeads (Fig. 2e) shows a band at 1587 cm^{-1}, whereas no such peak was observed in SA and PEG, confirmed the interaction between SA and PEG and also a band at 1066 cm^{-1} indicates the formation of microbeads. On comparing the FTIR spectra of placebo microbeads and drug loaded SA/PEG microbeads (Fig. 2f), the band at 1587 cm^{-1} in placebo microbeads was shifted to 1596 cm^{-1} in drug loaded SA/PEG microbeads, which confirmed that the drug interacts with the polymer matrix. The FTIR spectra of drug loaded SA/PEG/KA microbeads (Fig. 2g) shows characteristic bands similar to drug loaded SA/PEG microbeads, but the O – H stretching frequency was decreased due to interaction of KA with active sites of polymer molecules and also a new band appears at 902 cm^{-1}, which confirmed that the KA intercalates with active sites of polymer matrices and drug molecules[33].

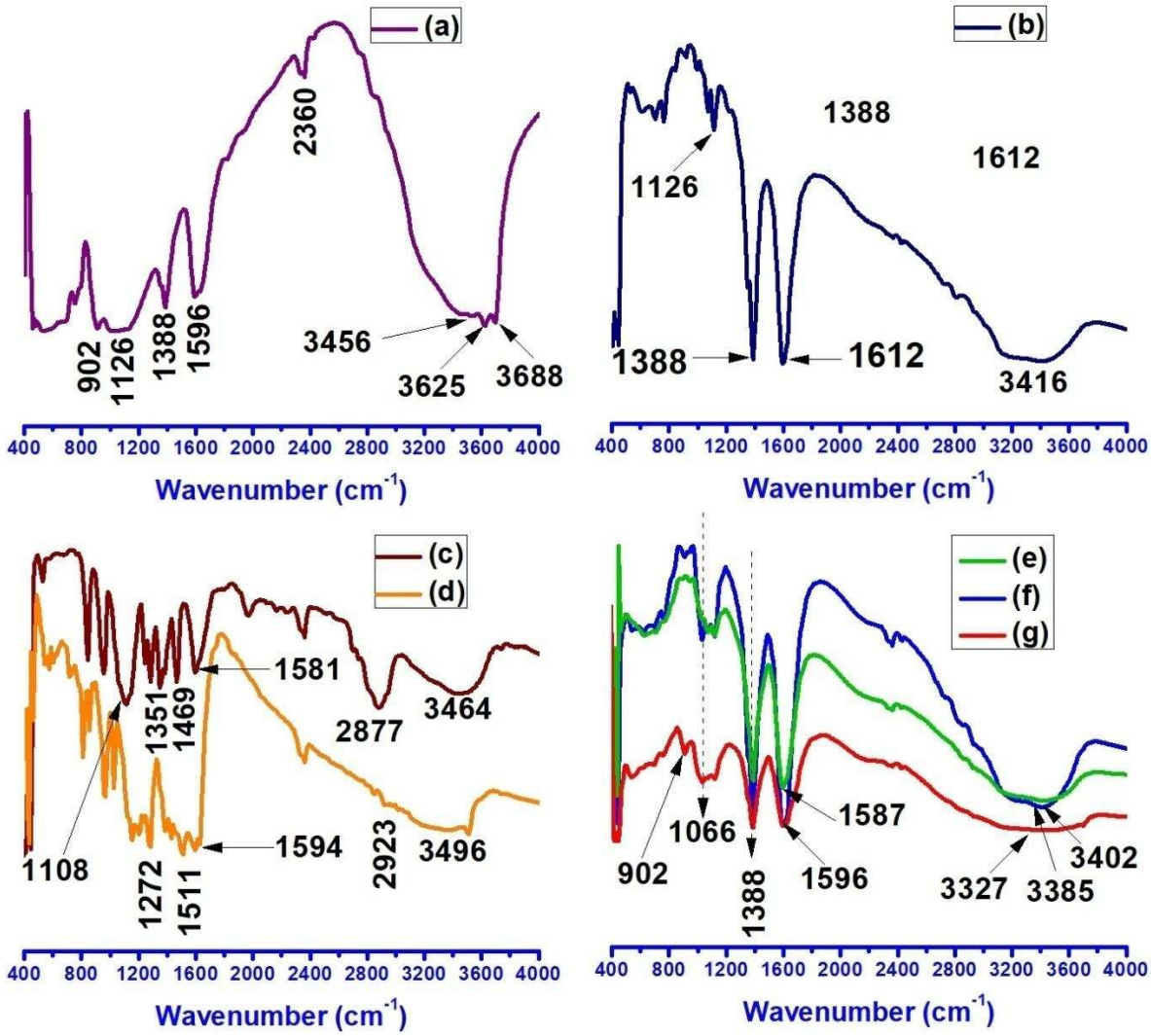

Fig.2. FTIR spectrum of pure KA (a), SA (b), PEG (c), CUR (d), placebo micro beads (e), drug loaded SA/PEG micro beads (f) and drug loaded SA/PEG/KA micro beads (g).

3.3. DSC Analysis

DSC thermograms of pure CUR (a), placebo microbeads (b) and drug loaded SA/PEG microbeads (c) are displayed in Fig. 3. The drug CUR (Fig. 3a) shows a sharp peak at 189 ^{o}C due to polymorphism and melting, but in the case of drug loaded SA/PEG microbeads (Fig. 3c) no such peak was observed at 189 ^{o}C, suggesting that the drug was uniformly dispersed in polymer matrices at molecular level.

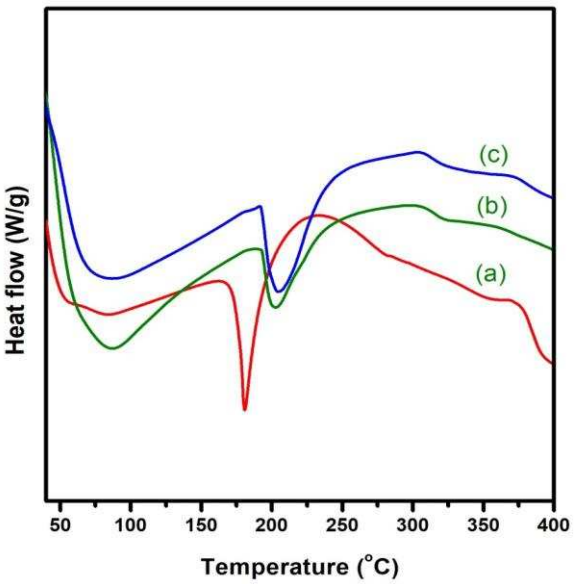

Fig.3. DSC curves of pure CUR (a), placebo microbeads (b) and drug loaded SA/PEG microbeads (SP3 Formulation) (c)

3.4. TGA Analysis

Fig. 4 shows the thermograms of Pure CUR (a), placebo microbeads (b), drug loaded SA/PEG microbeads (SP3 Formulation) (c), drug loaded SA/PEG/KA microbeads (d) and KA (e). The thermogram of KA (Fig. 4e), shows first mass los at 20-200 °C is due to moisture loss, the major weight loss step of KA was found in between the region of 450-600 °C is due to dehydroxylation of Kaolin and continue up to 900 °C to produce metakaolin. From the Fig. 4a, it was observed that the CUR curve should stable up to 169 °C and then its starts mass loss and being maximum at 393 °C due to total degradation of the compound. The thermal decomposition of placebo microbeads (Fig. 4b) follows three steps. The first weight loss step was found in between 40-187 °C with mass loss of 18% is due to the evaporation of adsorbed water. The second weight loss step was observed in between the region of 188-290 °C with mass loss of 14% due to the degradation of sodium alginate, followed by the mass loss of 10% in the region of 291-444 °C due to degradation remaining polymer network. In the case of drug loaded SA/PEG microbeads (Fig. 4c), the thermal decomposition follows four steps. The first mass loss of 17 % is observed in the region of 40-184 °C is due to the loss of moisture from the network. The second weight loss step was found in the region of 190-205 °C with mass loss of 11% due to the degradation of SA. The third weight loss of 11% in the region of 207-286 °C due to degradation of CUR and the last step was found in the region of 290-600 °C with the weight loss of 15% due to degradation of remaining polymer network. The thermal degradation of drug loaded SA/PEG/KA microbeads (Fig. 4d) follows four consecutive steps. The first with weight loss of 26% was found in the region of 40-182 °C due to the evaporation of adsorbed water in polymer network. The second and third step with weight loss of 10% and 9% in the region of 187-203 °C and 206-285 °C respectively is due to the degradation of SA and CUR. The final step was found in the region of 287-6200 °C with mass loss of 13% is ascribed to the degradation of remaining polymer network. From the results of TGA, it was concluded that drug loaded SA/PEG/KA polymer network shows an overall improvement in the thermal stability of microbeads.

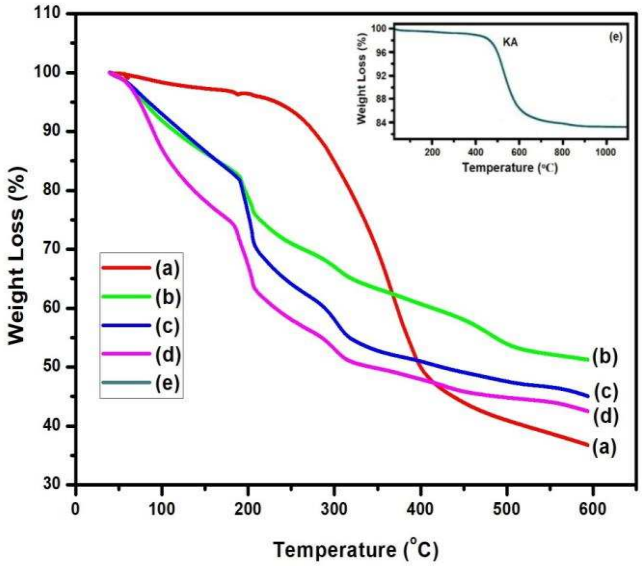

Fig.4. TGA curves of Pure CUR (a), placebo microbeads (b), drug loaded SA/PEG microbeads (SP3 Formulation) (c), drug loaded SA/PEG/KA microbeads (d) and KA (e)

3.5. XRD Analysis

X-ray diffraction studies were performed to investigate the crystalline behaviour of CUR and also confirm the intercalation of CUR with KA in the polymer network. The XRD patterns of CUR (a), placebo microbeads (b), drug loaded SA/PEG microbeads (c), KA (d) and drug loaded SA/PEG/KA microbeads (e) are displayed in Fig. 5. The most intensive peaks of CUR (Fig. 5a) were observed in the 2θ region of 12-28° suggesting its crystalline nature. But these peaks are not observed in drug loaded SA/PEG microbeads due to the absence of CUR crystals in the drug loaded SA/PEG (Fig. 5c) microbeads, hence confirmed that CUR is molecularly dispersed in the polymeric network. The XRD pattern of KA (Fig. 5.d) shows a characteristic peaks at 11.90°, 20.69° and 24.46° indicates the presence of kaoline. The peak at 26.60° confirms the presence of traces of quartz. The XRD pattern of drug loaded SA/PEG microbeads shows peaks at 12.52° and 20.25° which confirmed that the drug was intercalated with KA.

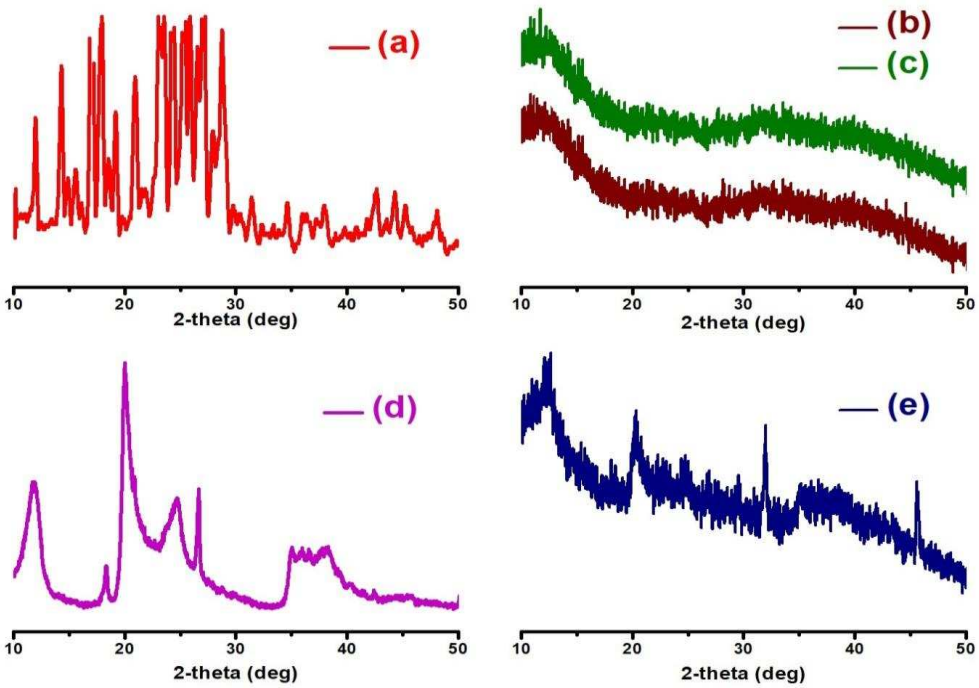

Fig.5. XRD patterns of CUR (a), placebo microbeads (b), drug loaded SA/PEG microbeads (SP3 Formulation) (c), KA (d) and drug loaded SA/PEG/KA microbeads (e)

3.6. SEM Analysis

Fig. 6 illustrates the topographical images of microbeads obtained under different blend polymer ratios. The outer surface of microbeads shows rough surface with visible wrinkles. It was interesting to see that more porous nature was observed in SP1 (Fig. 6a) due to formation of less rigid network of sodium alginate network. Whereas the formulations SP2 (Fig. 6b) and SP7 (Fig. 6d) shows less porous nature due to formation of rigid polymer network of SA/PEG. Fig. 6c shows the scanning electron micrograph of SP6, it was observed the outer surface was more rigid with rough surface, this confirmed the presence of KA platelets in the polymer network. From the results of SEM images, the bead size was measured as 1000 to 1300 µm.

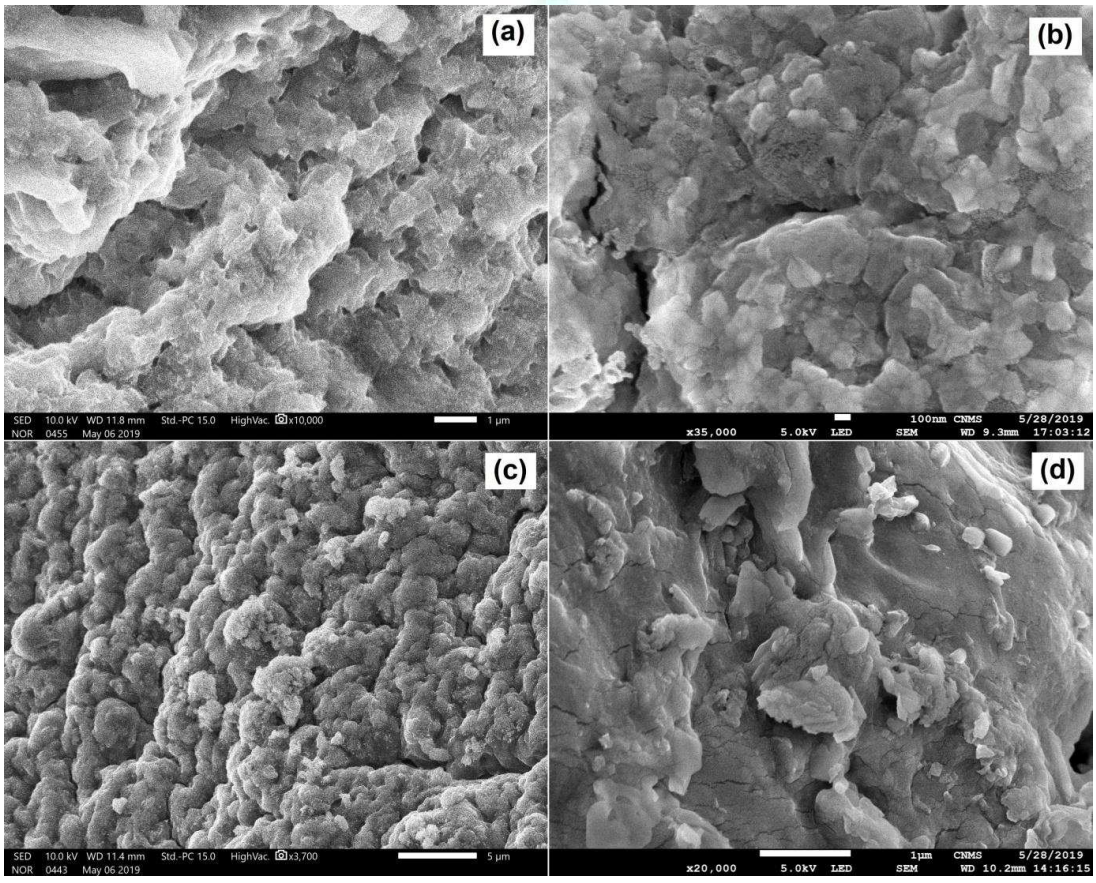

Fig. 6. SEM images of SP1 (a), SP2 (b), SP6 (c) and SP7 (d) microbeads

3.7. EDS Analysis

To find out the elemental composition of SP2 and SP6 formulations, EDS analysis were performed and the results are displayed in Fig. 7. The EDS spectra of SP2 (Fig. 7a) shows C, O, Na, Cl and Ca peaks, whereas these similar peaks were observed in SP7 (Fig. 7b), but along with these peaks Al, Si and K peaks were observed in SP7, which confirmed the presence of KA in microbeads.

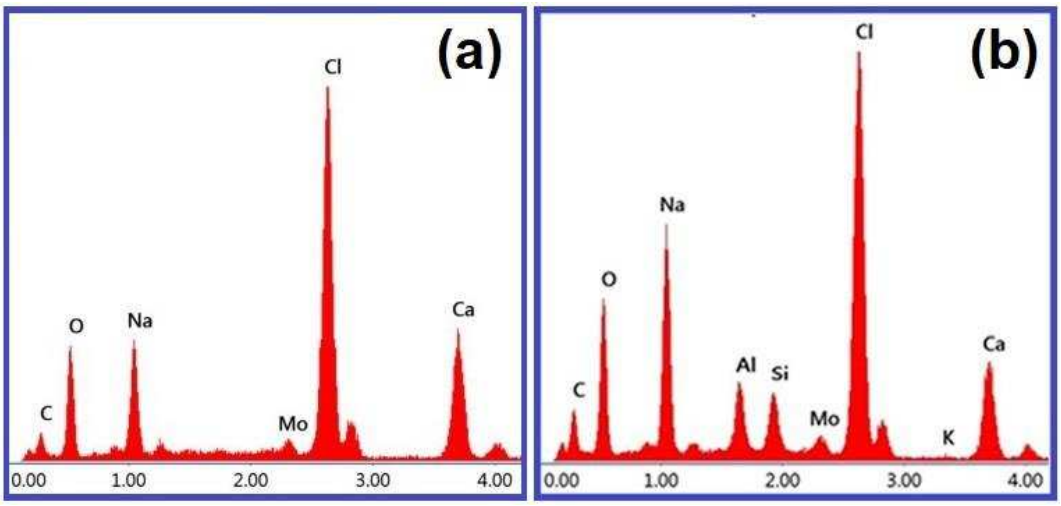

Fig. 7. EDS spectra of drug loaded SA/PEG microbeads (a) and drug loaded SA/PEG/KA microbeads (b)

3.8. Swelling measurements

Swelling degree is one of the most important factors of polymeric hydrogel beads for biomedical applications, because they show strong influence on diffusion of oxygen, drugs, nutrients and other water soluble metabolites. In order to investigate the swelling degree of microbeads, swelling experiments were performed in both pH 1.2 and 7.4 at 37°C and the results are displayed in Fig. 8. From the Fig. 8a and b, it was observed that the swelling degree was more in pH 7.4 than the pH 1.2. This is due to at pH 1.2 hydrogen bonding interactions were developed between –COOH groups of polymeric chains and solvent molecules resulting shrinking of network consequently the swelling ratio was observed to decrease[34]. While at pH 7.4 the carboxylic groups repel the water molecules because of the existence of ionic repulsions resulting the increasing of swelling degree. Therefore the developed beads are good promising carriers to deliver drug molecules at intestine and to avoid gastric release of drugs.

At pH 7.4 the swelling degree of all formulations was different due to the variation in blend composition of polymer network. From Fig. 8a, it was observed that swelling degree was decreased with the increase of PEG content in polymer network. This can be clarified by the SEM results. From the SEM studies it was observed that the porous nature was decreased with increase of PEG content in the polymer network. If the porous nature increases therefore it can accommodate more amount of water in their pores resulting in higher swelling degree. The swelling degree of SP4, SP5 and SP6 decreases with the increase of KA content in polymer network, this due to the formation of more rigid network, which restricted the inward flow of solvent molecules, resulting lower swelling degree.

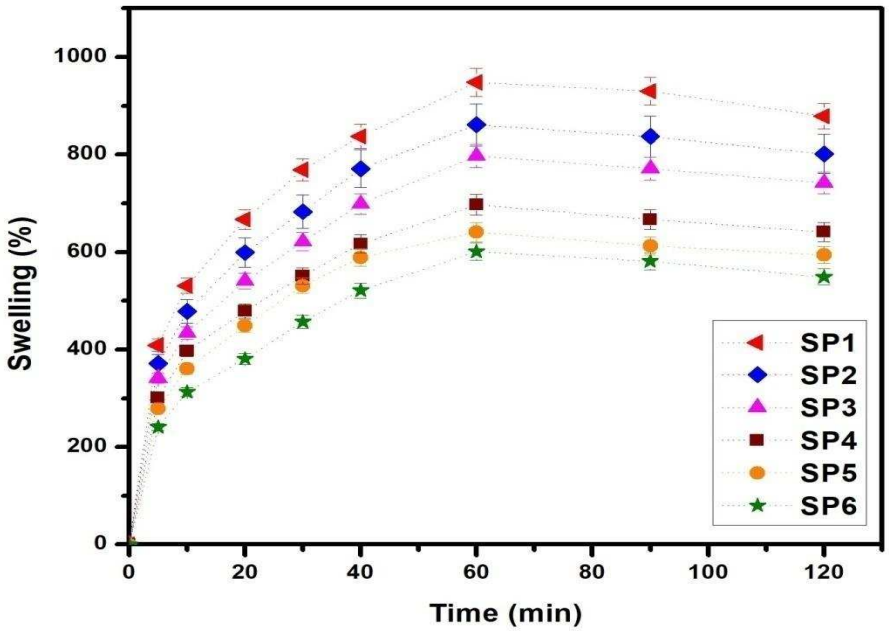

Fig. 8.a. Swelling studies in pH 7.4 at 37°C

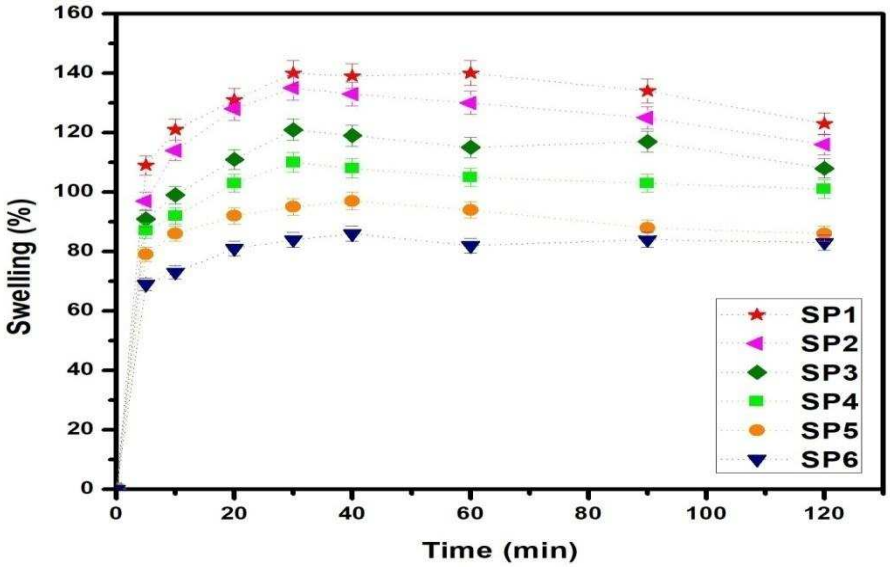

Fig. 8.b. Swelling studies in pH 1.2 at 37°C

3.9. Encapsulation Efficiency (%EE)

Encapsulation efficiency of drug loaded microbeads varied for all formulations due to variation in blend composition of polymer matrix and the results are listed in Table 2. The %EE was decreased with increase of PEG content in the polymer due to formation of more rigid network, thereby swell to less extent, which results low %EE values. This effect was observed in formulations of SP1, SP2 and SP3. As the concentration of KA increases in the polymer network %EE also increases this is due to KA has large specific area in its structure, good absorption capacity and develops hydrogen bonding between CUR and hydroxyl groups of KA.

3.10. In Vitro Drug Release Studies

The in vitro release studies of CUR from the microbeads were carried out under both pH 1.2 and 7.4 medium conditions and the release profiles for all formulations are displayed in Fig. 9a and b. The release data at pH 7.4 showed high release rate and avoid its release in acidic conditions pH 1.2. this is due to at pH 7.4, the carboxylate groups have less interactions with buffer medium therefore the network becomes more slack, hence the entrapped drug molecules easily leached out from the network. The obtained in vitro release results are correlated with the swelling results has previously discussed in this work.

At pH 7.4, the release rate was different for all profiles, this can be explained based on the composition of polymer network. The drug release profiles of SP1, SP2 and SP3 decreases as the content of PEG increases, this is due to formation of rigid network, hence CUR particles haven't chance to escape from the polymer network. The release rate of SP4, SP5 and SP6 decreases with the increase of KA content, this is due to the intercalated drug molecules cannot be exchanged completely in ion exchange process with phosphate ions of the buffer solution which leads to incomplete release process.

To understand the drug release mechanism of CUR from the blend microbeads, the in vitro release data was fitted in to the following Korsmeyer-Peppas kinetic equation

$$\frac{M_t}{M_\infty} = kt^n$$

where M_t/M_α is a fraction of the drug released at time t, k is the rate constant, and n is the release exponent which represents the release mechanism. The values of n are obtained in the range of 0487-0.529 and the values are listed Table 2, the results suggesting that the release followed non-Fickian type diffusion process.

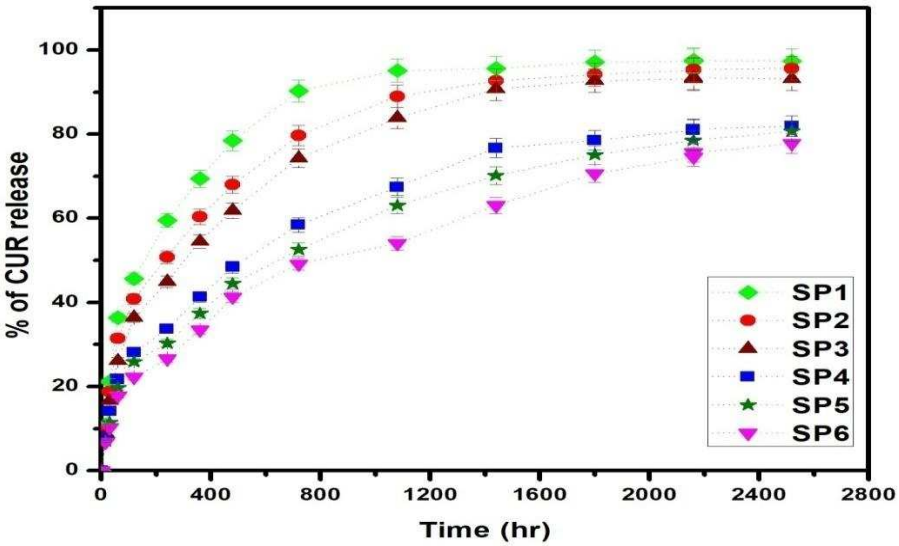

Fig. 9.a. % CUR release in pH 7.4 at 37 °C

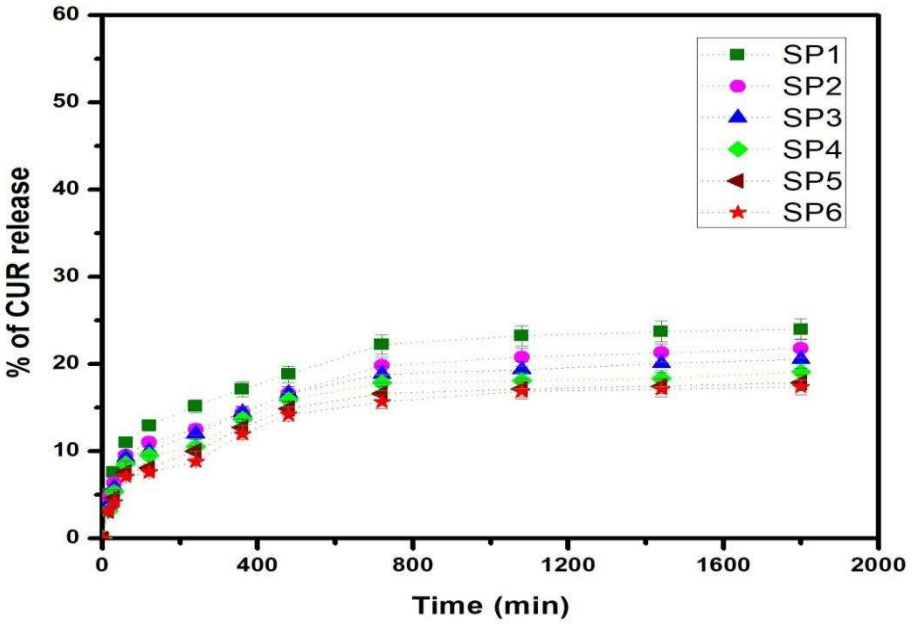

Fig. 9.b. % CUR release in pH 1.2 at 37 °C

Table 2. Release kinetics parameters at pH-7.4 and encapsulation efficiency (%EE) of all samples

Formulation code	pH 7.4			%EE
	r^2	n	k	
SP1	0.942	0.524	0.1398	45.16
SP2	0.948	0.517	0.1216	42.21
SP3	0.961	0.529	0.0950	40.32
SP4	0.958	0.483	0.0845	43.41
SP5	0.962	0.498	0.0818	46.32
SP6	0.970	0.487	0.0608	49.51

4.0. CONCLUSION

In this study, we fabricated CUR encapsulated semi IPN micro beads from SA/PEG/KA through simple ionotropic gelation method. The developed microbeads were confirmed by FTIR spectroscopy. Thermal stability and molecular level dispersion of CUR in microbeads were confirmed by TGA and DSC respectively. Intercalation of CUR with KA was confirmed by XRD studies. From the SEM pictures it was observed that the microbeads are spherical in shape and wrinkled surface with few depressions on the surface and also it confirmed the presence of KA platelets on outer surface of microbeads. From the SEM results the average diameter of microbeads was found to be 1000 to 1300 µm. The dynamic swelling studies were depended on the blend composition and pH of the medium. Swelling degree was decreased with the increase of PEG and KA content in polymer network. The *in vitro* release studies were performed in both pH 1.2 and 7.4 at 37°C and the results were fitted into peppas equation, which confirmed that the maximum % CUR release (96%) was achieved to 42 h via diffusion controlled non-Fickian transport.

Acknowledgements

Research support provided by the department of Chemistry, S.K. University, Ananthapuramu, Andhra Pradesh, India.

Financial support and sponsorship: Nil

Conflict of Interests: The authors have indicated that they have no conflicts of interest regarding the content of this article.

REFERENCES

1. Zhang W, Ding Y, Boyd SA, Teppen BJ, Li H. Sorption and desorption of carbamazepine from water by smectite clays, Chemosphere, 2010; 81:954–960.
2. Massaro M, Colletti CG, Lazzara G, SRiela S, The Use of Some Clay Minerals as Natural Resources for Drug Carrier Applications, Journal of Functional Biomaterials, 2018, 9:58-79.
3. Isabel Carretero M, Manuel Pozo, Clay and non-clay minerals in the pharmaceutical industry Part I. Excipients and medical applications, Applied Clay Science, 2009; 46:73-80.
4. López-Galindo A, Viseras C, Aguzzi C, Cerezo P, Pharmaceutical and Cosmetic Uses of Fibrous Clays, Developments in Clay Science, 2011, 3:299-324.
5. Carretero M.I., Gomes C.S.F., Tateo F., Clays, Drugs, and Human Health. Developments in Clay Science, 2013; 5:711-764.
6. Chávez-Delgado M.E., Kishi-Sutto C.V., La-Riva X.N.A.D., Rosales-Cortes M., Gamboa-Sánchez P., Topic usage of kaolin-impregnated gauze as a hemostatic in tonsillectomy, Journal of Surgical Research, 2014; 192:678-685.
7. Hu P.W., Yang H.M., Insight into the physicochemical aspects of kaolins with different morphologies, Applied Clay Science, 2013; 74:58-65.
8. Liang Y, Xu C, G. Li, T. Liu, J.F. Liang, X. Wang, Graphene-kaolin composite sponge for rapid and riskless hemostasis, Colloids and Surfaces B: Biointerfaces, 2018; 169:168-175.
9. Sena M.J., Douglas G., Gerlach T., Grayson J.K., Pichakron K.O., D. Zierold, A pilot study of the use of kaolin-impregnated gauze (Combat Gauze) for packing high-grade hepatic injuries in a hypothermic coagulopathic swine model, Journal of Surgical Research, 2013; 183:704-709.
10. Myung Hun Kim, Goeun Choi, Ahmed Elzatahry, Ajayan Vinu, Young Bin Choy, Jin-Ho Choy, Review of clay-drug hybrid materials for biomedical applications: administration routes, Clays and Clay Minerals, 2016; 64(2):115-130.

11. Zhu L., Zhang L., Tang Y., D. Ma, J. Yang, Synthesis of kaolin/sodium alginate-grafted poly(acrylic acid-co-2-acrylamido-2-methyl-1-propane sulfonic acid) hydrogel composite and its sorption of lead, cadmium, and zinc ions, Journal of Elastomers & Plastics, 2015; 47(6):488-501.
12. Sanchez-Ballester N.M., Soulairol I., Bataille B., Sharkawi T., Flexible heteroionic calcium-magnesium alginate beads for controlled drug release, Carbohydrate Polymers, 2019; 207:224-229.
13. Borges O., Cordeiro-da-Silva A. , Romeijn S.G. , Amidi M., de Sousa A., Borchard G, Junginger H.E., Uptake studies in rat Peyer's patches, cytotoxicity and release studies of alginate coated chitosan nanoparticles for mucosal vaccination, Journal of Controlled Release, 2006; 114(3):348-358.
14. Lee K.Y., Mooney D.J., Alginate: properties and biomedical applications, Progress in Polymer Science, 2012; 37(1):106-126.
15. Subhraseema Das and Usharani Subuddhi, Controlled Delivery of Ibuprofen from Poly(vinyl alcohol)–Poly(ethylene glycol) Interpenetrating Polymeric Network Hydrogels, Journal of Pharmaceutical Analysis, 2019; 9(2):108-116.
16. Anisha A. D'souza & Ranjita Shegokar, Polyethylene glycol (PEG): a versatile polymer for pharmaceutical applications, Expert Opinion on Drug Delivery, 2016 13(9):1257-75.
17. Bing-Liang Ma, Yan Yang, Yan Dai, Qiao Li, Ge Lin, Yue-Ming Ma, Polyethylene glycol 400 (PEG400) affects the systemic exposure of oral drugs based on multiple mechanisms: taking berberine as an example, RSC Advances, 2017; 7:2435-2442.
18. Bendels S., Tsinman O., Wagner B., D. Lipp, I. Parrilla, M. Kansy, A. Avdeef, PAMPA-Excipient Classification Gradient Map, Pharmaceutical Research, 2006; 23(11):2525-2535.
19. Parlato M., Reichert S., N. Barney, et al., Poly(ethylene glycol) hydrogels with adaptable mechanical and degradation properties for use in biomedical applications, Macromolecular Bioscience, 2014; 14:687-698.
20. Lin C.C., K. S. Anseth, PEG hydrogels for the controlled release of biomolecules in regenerative medicine, Pharmaceutical Research, 2009; 26:631-643.
21. Wang Q., N. Zhang, X. Hu, et al., Alginate/polyethylene glycol blend fibers and their properties for drug controlled release, Journal of Biomedical Materials Research Part A, 2007; 82:122-128.
22. Bisht S., and Maitra A., Systemic Delivery of Curcumin: 21st Century Solutions for an Ancient Conundrum, Current Drug Discovery Technologies, 2009; 6:192-199.
23. Srimal R. C., Dhawan B. N., Pharmacology of diferuloyl methane (curcumin), a non-steroidal anti-inflammatory agent, Journal of Pharmacy and Pharmacology, 1973; 25:447-452.
24. Ruby A.J., G.Kuttan, K.Dinesh Babu, K.N.Rajasekharan, R.Kutta, Anti-tumour and antioxidant activity of natural curcuminoids, Cancer Letters, 1995; 94(1):79-83.
25. Kim M.K., Choi G.J., H.S. Lee, Fungicidal property of Curcuma longa L. rhizome-derived curcumin against phytopathogenic fungi in a greenhouse, Journal of Agricultural and Food Chemistry, 2003; 51(6):1578-1581.
26. Deodhar S.D., Sethi R., Srimal R.C., Preliminary study on antirheumatic activity of curcumin (diferuloyl methane), Indian Journal of Medical Research, 1980; 71:632-634.
27. Srivastava R., M. Dikshit, R.C. Srimal & B.N. Dhawan, Anti-thrombotic effect of curcumin, Thrombosis Research, 1985; 40:413-417.
28. Aggarwal B.B., S. Banerjee, U. Bharadwaj, B. Sung, S. Shishodia, G. Sethi, Curcumin induces the degradation of cyclin E expression through ubiquitin-dependent pathway and up-regulates cyclin-dependent kinase inhibitors p21 and p27 in multiple human tumor cell lines, Biochemical Pharmacology, 2007; 73:1024-1032.
29. Chen H.W., Huang H.C., Effect of curcumin on cell cycle progression and apoptosis in vascular smooth muscle cells. British Journal of Pharmacology, 1998; 124:1029-1040.
30. Rekik S.B., Gassara S., Bouaziz J., A. Deratani, S. Baklouti, Development and characterization of porous membranes based onkaolin/chitosan composite, Applied Clay Science, 2017; 143:1-9.
31. Shameli K, Ahmad M.B., Jazayeri S.D., Sedaghat S, Shabanzadeh P, H. Jahangirian, M. Mahdavi, Y. Abdollahi, Synthesis and Characterization of Polyethylene Glycol Mediated Silver Nanoparticles by the Green Method, International Journal of Molecular Sciences, 2012; 13:6639-6650.
32. Madhusudana Rao K, Krishna Rao K.S.V., Ramanjaneyulu G., Chang-Sik Ha, Curcumin encapsulated pH sensitive gelatin based interpenetrating polymeric network nanogels for anti cancer drug delivery, International Journal of Pharmaceutics, 2015; 478:788-795.
33. Zhang Y, Long M, Huang P, Yang H, Chang S, Hu Y, Tang A, Mao L. Intercalated 2D nanoclay for emerging drug delivery in cancer therapy. Nano Research, 2017; 10:2633-2643.
34. Eswaramma S, K.S.V. Krishna Rao, Synthesis of dual responsive carbohydrate polymer based IPNmicrobeads for controlled release of anti-HIV drug, Carbohydrate Polymers, 2017; 156:125-134.